Integrative Biology

Cite this: *Integr. Biol.*, 2011, **3**, 1179–1187

www.rsc.org/ibiology

PAPER

Spatially organized *in vitro* models instruct asymmetric stem cell differentiation†

Yi-Chin Toh,[ac] Katarina Blagovic,[a] Hanry Yu[cdefghi] and Joel Voldman*[ab]

Received 21st September 2011, Accepted 22nd September 2011
DOI: 10.1039/c1ib00113b

Understanding developmental biology requires knowledge of both the environmental factors regulating stem cell differentiation, which are increasingly being defined, and their spatial organization within a structurally heterogeneous niche, which is still largely unknown. Here we introduce spatially organized stem cell developmental models to interrogate the role of space in fate specification. Specifically, we developed Differential Environmental Spatial Patterning (δESP) to organize different microenvironments around single embryonic stem cell (ESC) colonies *via* sequential micropatterning. We first used δESP to decouple and understand the roles of cell organization and niche organization on ESCs deciding between self-renewal and differentiation fate choices. We then approximated *in vitro* an embryonic developmental step, specifically proximal–distal (PD) patterning of the mouse epiblast at pre-gastrulation, by spatially organizing two extraembryonic environments around ESCs, demonstrating that spatial organization of these three cell types is sufficient for PD patterns to form *in vitro*.

[a] *Research Laboratory of Electronics, Massachusetts Institute of Technology, 77 Massachusetts Ave, Cambridge, MA 02139, USA*
[b] *Department of Electrical Engineering and Computer Science, Massachusetts Institute of Technology, 77 Massachusetts Ave, Cambridge, MA 02139, USA. E-mail: voldman@mit.edu*
[c] *Institute of Bioengineering and Nanotechnology, A*STAR, 31 Biopolis Way, #04-01, Singapore 138669, Singapore*
[d] *Department of Physiology, Yong Loo Lin School of Medicine, National University of Singapore, MD 9 #03-03, 2 Medical Drive, Singapore 117597, Singapore*
[e] *Mechanobiology Institute, Temasek Laboratories, National University of Singapore, #05-01, 5A Engineering Drive 1, Singapore 117411, Singapore*
[f] *NUS Graduate School for Integrative Sciences and Engineering, Centre for Life Sciences (CeLS), #05-01, 28 Medical Drive, Singapore 117456, Singapore*
[g] *Singapore-MIT Alliance Research and Technology, National University of Singapore, S16-05-08, 3 Science Drive 2, Singapore 117543, Singapore*
[h] *NUS Tissue-Engineering Program, DSO Labs, National University of Singapore, Singapore 117597, Singapore*
[i] *Department of Mechanical Engineering, Massachusetts Institute of Technology, Cambridge, MA 02139, USA*
† Electronic supplementary information (ESI) available: See DOI: 10.1039/c1ib00113b

Introduction

One goal of developmental biology is to understand how organized stem cell differentiation arises. The emergence of differentiation patterns in many developmental processes are underpinned by asymmetries in the stem cell microenvironment.[1,2] For instance, surgical disruption of structural asymmetry (removal of extraembryonic ectoderm) in gastrulating embryos disrupts normal body axis patterning and subsequent mesoderm development.[3] Similarly, the choice for an adult stem cell to self-renew or differentiate depends on its location within a structurally asymmetric niche.[2]

Traditional developmental biology takes a reductionist approach to break down the process into discrete functional steps, such as embryonic stages. The microenvironmental asymmetries in each stage are then characterized at the tissue and cellular level[1,4] in model organisms *e.g.*, *C. elegans*[5] and mouse,[1,6] where spatial organization of multiple microenvironments is inherently present. With the advent of transgenic and knock-out animals, these steps are increasingly being defined chemically to identify important molecules and interactions at a

Insight, innovation, integration

The importance of spatial information from the microenvironment on the fate of stem cells has been widely acknowledged. However, relying on *in vivo* models to study development faces limitations that are both technical (experimental accessibility of individual cells) and theoretical (the *proportion* and *organization* of multiple environmental constituents within a niche cannot be determined easily). Therefore there is a compelling need to develop alternative models to examine spatial issues in developmental processes. Here we report the first method to reconstitute stem cell differentiation patterns *in vitro* that are representative of a developmental step. We achieved this by imposing direct control over the organization of multiple stem cell microenvironments using sequential, aligned micropatterning, which in turn spatially directs stem cell differentiation.

given developmental stage.[1,6,7] There have also been substantial efforts to employ *in vitro* stem cell models to identify other environmental signals, such as mechanical forces and extracellular matrices (ECMs), that modulate various differentiation fates.[8–10] Although there is increasing knowledge in the instruction of stem cells to adopt various fates, for example, mesoderm and ectoderm lineages *via* environmental factors,[11] we are still unable to address *organizational* questions, such as why mesoderm development always occurs at a specific location relative to ectoderm *in vivo*.[1] To ultimately understand and control developmental processes, we need to determine the minimal collation of factors sufficient for spatially organized differentiation to emerge and how they interact with each other spatially. However, the irreducibly complex nature of an entire organism makes it experimentally impractical to manipulate multiple environmental factors simultaneously to probe questions of spatial organization or sufficiency *in vivo*.[11]

To create spatially organized *in vitro* developmental models, one must independently pattern stem or progenitor cells in the appropriate developmental niche, which itself may consist of multiple spatially organized cells and ECMs. Traditional monolayer stem cell cultures and embryoid bodies do not allow spatial control,[8,12] whereas cell micropatterning techniques (*e.g.*, microcontact printing[9,13]) are not suitable for creating spatially organized developmental models because they typically only allow coincident patterning of cells and niche within the same spatial locality (*e.g.*, a patch of cells directly on a patch of ECM),[14] are limited in their ability to pattern >2 cell types at once[14,15] (and thus the complexity of the niche), and/or physically constrain cells thus preventing normal outgrowth and differentiation.[13,16] To develop *in vitro* spatially organized models, here we developed a multi-component micropatterning technique, which we termed Differential Environmental Spatial Patterning (δESP), that allows successive alignment and patterning of different microenvironments independently of stem cell colonies. This method combines two micropatterning steps *i.e.*, stencil[17] and Bio Flip Chip (BFC)[16] in a novel manner to independently but controllably pattern a microenvironmental niche and the stem cells within it.

To demonstrate the power of spatially organized *in vitro* models, we addressed two questions in stem cell and developmental biology. We first used δESP to determine whether extrinsically imposed local microenvironments can alter ESC fate specification. Prior stem cell micropatterning work alluding to this phenomenon[13,18] could only alter the colony size and thus could not decouple spontaneous cell organization from environmental (ligand) organization because the cells themselves produce the ligands (*i.e.*, a circular pattern of cells creates a circular pattern of ligand; a high density of cells results in a high concentration of ligand), and thus only allow for emergent organization.

We next investigated a question in early development surrounding sufficiency of factors for patterning. The initiation of germ layer formation in mouse begins around E5.5 with the patterning of epiblast (comprising of pluripotent cells that eventually differentiate into all tissues of the new organism) along a proximal-distal (PD) axis that is underpinned by two juxtaposed extraembryonic tissues (*i.e.*, extraembryonic ectoderm (ExE) and the visceral endoderm (VE)).[1,4] This differentiation pattern has been well characterized and readily defined molecularly,[1,4] but no one has formally examined whether simple organization of proteins and cells alone would be able to generate a PD axial pattern or whether other factors are required. To investigate this system, we created a synthetically organized version of the embryo at that stage consisting of two different microenvironments representative of the extraembryonic tissues organized around a colony of embryonic stem cells (ESCs) (Fig. 1A). Using this model, we generated for the first time an *in vitro* PD pattern in the differentiating colonies, which we quantified spatially by proximal embryonic markers Wnt3a, T, Cripto1, and Fgf8. We further demonstrated that the emergent PD pattern is partly modulated by Wnt signaling gradient established by the asymmetric microenvironment. The ability to generate spatially organized *in vitro* developmental models in a configurable and reproducible manner will have significant impact on basic developmental biology research and drug teratogenicity testing.

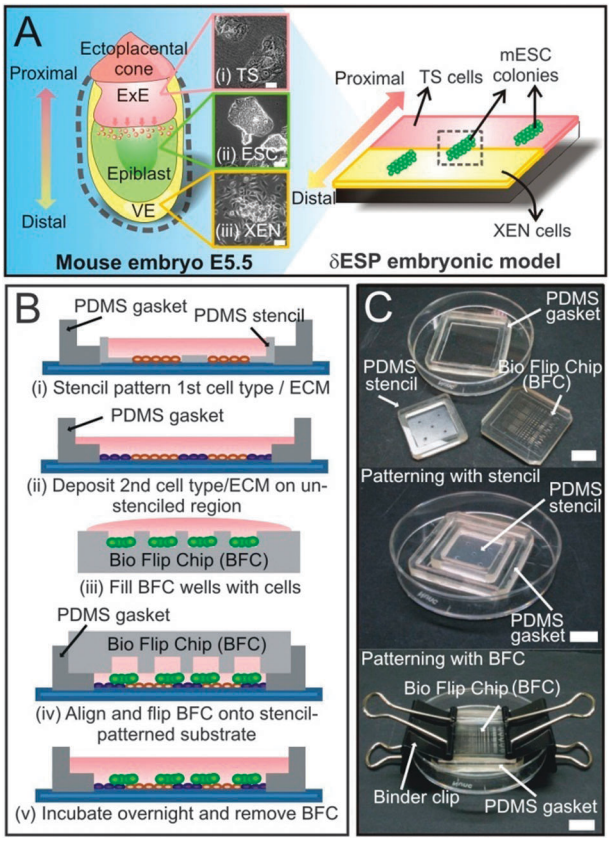

Fig. 1 Reconstituting proximal-distal (PD) epiblast patterning *in vitro* with Differential Environmental Spatial Patterning (δESP). (A) Conceptual design. (B) Operation of δESP. (C) Components and assembly of δESP; middle and bottom panels show the assembly of components during the stenciling and flipping steps of δESP respectively. Scale bar = 1 cm.

Results

Spatial organization of microenvironments around stem cell colonies with Differential Environmental Spatial Patterning (δESP)

To create a spatially organized *in vitro* developmental model, we developed Differential Environmental Spatial Patterning (δESP) to spatially organize different microenvironments (or niches)

around single stem cell colonies. We achieved this by using successive patterning steps to first create different microenvironments, and then position colonies of stem cells at the interface of the different microenvironments (Fig. 1B). First, stencil micropatterning was employed to generate dual microenvironments using a combination of different cells, cell/ECM, or different ECMs (Fig. 1Bi-ii, SI Fig. 1A). During the second step, we used Bio Flip Chip (BFC)[16] cell patterning to arrange stem cell aggregates of different sizes onto the stenciled substrate (Fig. 1Biii-iv, SI Fig. 1B–D). By aligning the stenciled micropatterns with the BFC wells using a PDMS stepped gasket (Fig. 1C, SI Fig. 1*E*), we can selectively position the stem cell aggregates such that they span across the interface of the stenciled microenvironments. In this fashion, we can create a multicomponent spatially organized niche and then independently pattern the stem cells with respect to that niche.

Emergence of stem cell differentiation patterns is instructed by spatially organized local microenvironments

We first applied the spatially organized *in vitro* developmental model to understand whether microenvironmental organization or cell organization instructs pluripotent stem cell fate in heterogeneous cultures. Spatial environmental heterogeneity exists in both bulk human and mouse ESC cultures as local self-renewal-supporting and non-supporting niches. This heterogeneity has been correlated to spatial variation in cell fates, which can be modulated by controlling the size of the colonies.[13,18] However, when studying this heterogeneity by varying colony size, the microenvironment emerges from the ESCs, coupling cell phenotype organization with microenvironment organization, and thus is unable to provide a definitive interpretation of whether cell fate patterning is indeed modulated by microenvironment heterogeneity.[1,19] Decoupling the two modes of organization with an imposed extrinsic environmental pattern allows more direct interpretation of the causal relationship between the microenvironment and cell fate.

To investigate whether imposed asymmetries in microenvironment organization would delineate the spatial pattern of reciprocal cell fates, we used δESP to selectively present self-renewing and differentiating microenvironments to mouse ESC (mESC) colonies. Culture of mESCs in serum-free (N2B27) basal medium with the proteins Leukemia Inhibitory Factor (LIF) and Bone Morphogenic Protein-4 (BMP4) is sufficient for maintaining self-renewal, whereas culture in basal medium alone induces neuroectodermal differentiation.[20,21] Feeder cells, such as mouse embryonic or STO fibroblasts traditionally used to maintain mESC cultures, act as sources for these proteins.[22] Indeed, when bulk-cultured in N2B27, STO fibroblasts maintained a self-renewing microenvironment for mESCs (SI Fig. 2A) while culture on gelatin allowed mESCs to differentiate into neuroectoderm (SI Fig. 2B).

We presented single mESC colonies with two defined microenvironments (*i.e.*, STO/N2B27 and gelatin/N2B27) and assessed how the local environment influences cell fate decisions (Fig. 2A). Alignment of the mESC colonies at the STO/gelatin interface was achieved by tracking the stabilized patterned interface and designing BFC wells at specific locations corresponding to the interface position on the substrate (SI Fig. 2C–D). Internal controls

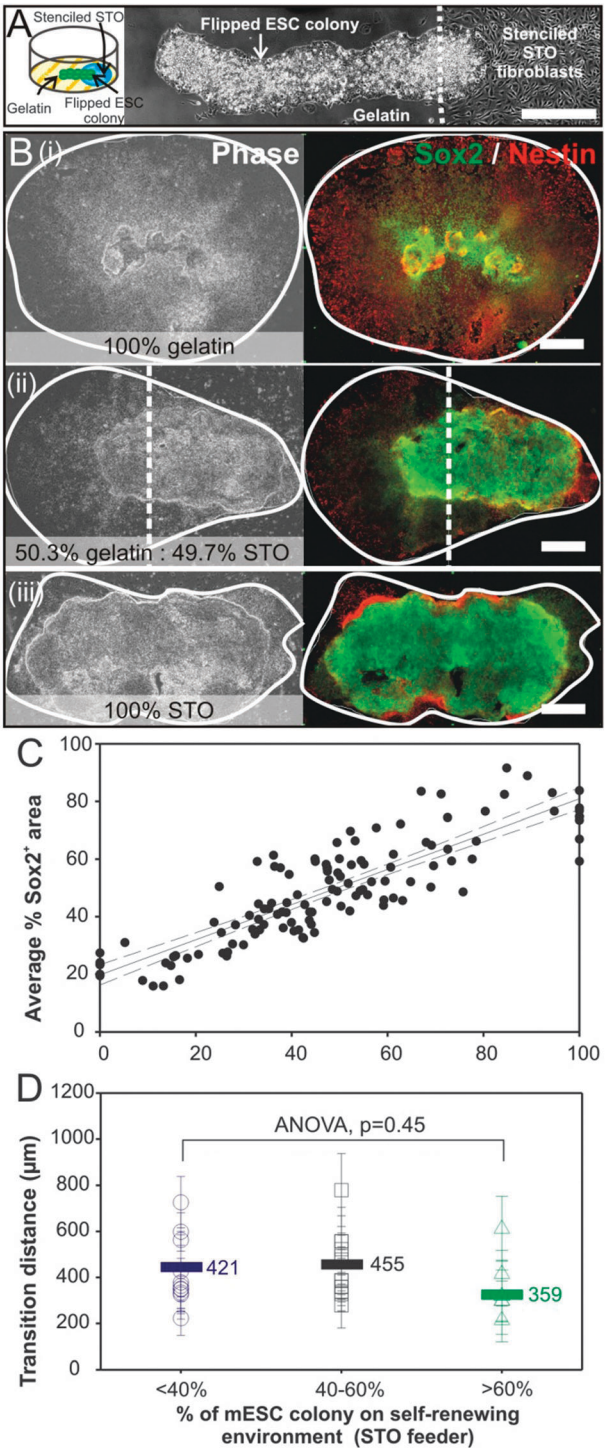

Fig. 2 Reciprocal cell fate patterning. (A) A mESC colony patterned on gelatin/STO fibroblast interface. (B) Expression of self-renewal ($Sox2^+$) and neural precursor ($Nestin^+$) markers after 5 days of culture. Colonies patterned on (i) gelatin alone, (ii) gelatin/STO interface and (iii) STO alone. (C) Control over average Sox2 expression by tuning the ratio of dual microenvironments. (D) Transition distance from a self-renewing ($Sox2^{high}$) to a differentiated phenotype ($Sox2^{low}$). Colonies were binned according to the ratios of dual microenvironments presented. Each data point represents the average transition distance for a colony ± s.e.m of 5 different profiles offset by 30°–60° from the long axis of a colony. Scale bars = 500 μm.

were generated by patterning colonies on STO or gelatin alone in the same culture dish. After 5 days of culture, we observed that expression of self-renewal (Sox2) and neural precursor (Nestin) markers was spatially distributed coincident with the patterned microenvironments (Fig. 2B). mESCs in colonies presented with a differentiating environment (on gelatin) alone expressed Nestin (Fig. 2Bi) in a radial symmetric manner, with a central region still expressing Sox2. This is consistent with observations that spatial patterns of differential cell fates develop autonomously even in a uniform extrinsic environment.[13] Similarly, colonies in a self-renewing environment (on STO cells) alone expressed Sox2 predominantly (Fig. 2Biii).

Colonies that were presented with both microenvironments (on STO/gelatin interface) exhibited asymmetric differentiation with an axis perpendicular to the interface (Fig. 2Bii). The pattern of the reciprocal phenotypes (*i.e.*, $Sox2^+$ self-renewing cells and $Nestin^+$ neural precursors) within a colony could be controlled by the relative extent of the two microenvironments presented (assessed by the percentage of colony area on STO cells). By patterning mESC colonies with increasing ratios of STO cells to gelatin, we could vary Sox2 expression within the colony between 20–80% (Fig. 2C) with a linear correlation between input differential microenvironments and resulting cell phenotype ($R^2 = 0.75$, $p = 0.0001$). When we examined the localization of different phenotypes within a mESC colony, we found that self-renewal and neuroectoderm phenotypes corresponded to the colony regions on STO cells and gelatin respectively (SI Fig. 3).

To show that the presented dual microenvironments modulate the cell fate pattern but do not influence the intrinsic differentiation processes (*e.g.*, kinetics of cell differentiation), we interrogated the interface over which mESCs switched between self-renewal and neuronal fates when presented with varying ratios of STO cells and gelatin. By tracing Sox2 expression along multiple designated axes originating from the center of the mESC colony, we obtained profiles describing a transition between self-renewing and differentiated phenotypes (SI Fig. 4). The phenotypic transition occurred over an average distance of ~400 μm, and was independent of the relative direction to the STO/gelatin interface, or of the ratios of STO cells to gelatin being presented (Fig. 2D). Since changing the input environmental organization alters the cell fate patterns (Fig. 2C) but not the boundary width of the phenotype transition, which is indicative of the length scales over which differentiation occurred, it is likely that intrinsic cellular regulation of cell fate remained relatively constant. By independently patterning stem cells and their niche, our results suggest that cell fate instruction is dominated by microenvironment heterogeneity.

Spatial localization of Wnt signaling modulates *in vitro* proximal-distal patterning of an ESC colony

Since imposed microenvironment organization can robustly direct differentiation patterns, we next examined the question of whether spatially organizing cells of extraembryonic *i.e.*, extraembryonic ectoderm (ExE) and visceral endoderm (VE), lineages in a PD orientation relative to a colony of mESCs (*in vitro* surrogate for inner cell mass), similar to how those tissues are organized in the embryo, would be sufficient for inducing molecular patterns akin to the embryonic PD axis (Fig. 1A). We first stenciled trophoblast stem (TS) cells, an ExE precursor cell line,[23] in strips and back-filled the remaining substrate with extraembryonic endoderm (XEN) cells, a primitive endoderm-derived cell line[24] (Fig. 3A). TS and XEN cells formed a well-defined interface (Fig. 3B), which remained stable for up to one week (SI Fig. 5A). We then used δESP to pattern mESC colonies on the TS-XEN interface (Fig. 3C). The TS/XEN/mESC co-culture was maintained in TS medium supplemented with anti-LIF antibody to allow for mESC differentiation over a period of up to 5 days (Fig. 3D, SI Fig. 5B–F).

To molecularly determine establishment of PD patterning, we assessed the distribution of putative proximal embryonic markers. These include Wnt3a and Brachyury (T) that are expressed in both the proximal extraembryonic tissues and epiblast,[25] as well as Cripto1 (a co-receptor of Nodal), Fgf8 and Lefty2 (a Nodal inhibitor), which are initially uniformly distributed throughout the epiblast but gradually localize to the proximal region at the onset of gastrulation.[6,7] We found that the mESC colonies acquired marker expression over time regardless of their underlying microenvironment (SI Fig. 6). Instructing differentiation by patterning control colonies entirely on TS or XEN cells alone resulted in symmetrical expression of Wnt3a, T, Cripto1, and Fgf8 (Fig. 3E).

We then asked whether colonies patterned across the TS-XEN interface would exhibit marker polarization, or whether other factors might be required for patterning to arise. Remarkably, mESCs patterned across the interface did indeed differentiate asymmetrically along the designated PD axis. For example, Wnt3a and T were highly expressed in the periphery of the colony on TS cells but were only weakly expressed in the region on XEN cells (Fig. 3F–G). Cripto1 and Fgf8 were also polarized, but in an opposite direction to Wnt3a and T (*i.e.*, higher in XEN cell region) (Fig. 3H–I). Intriguingly, in 20–30% of the colonies, we observed a graded PD expression of Cripto1 and Fgf8 within the region on XEN cells (Fig. 3H(ii), I(II), J). We did not observe significant polarization of Lefty2 when compared to control colonies (SI Fig. 7). This was expected because Lefty2 localization requires Lefty1 regulation, which is produced from the anterior visceral endoderm (AVE), a more mature developmental structure.[26] Taken together, these data suggest that a day-5 δESP embryonic model mimics a pre-implantation embryo that just initiated axis formation. mESCs on TS cells have acquired extraembryonic fates, since they expressed strongly for Wnt3a and T but only weakly for Cripto1 and Fgf8. mESCs patterned on XEN cells acquired an epiblast-like fate with graded patterning along the designated PD axis. The fact that all patterned colonies showed polarization of Wnt3a and T in the TS cell region but only a fraction exhibited graded patterning of Cripto1 and Fgf8 within the XEN cell region imply that the sequence of molecular patterning events in the δESP embryonic model is consistent with embryonic development *in vivo*—Cripto1 and Fgf8 function downstream of Wnt and T[1].

Since polarization of Wnt3a and T was consistently observed, we quantified their intensities in the respective colony regions on TS and XEN cells. The resultant proximal (on TS cells)

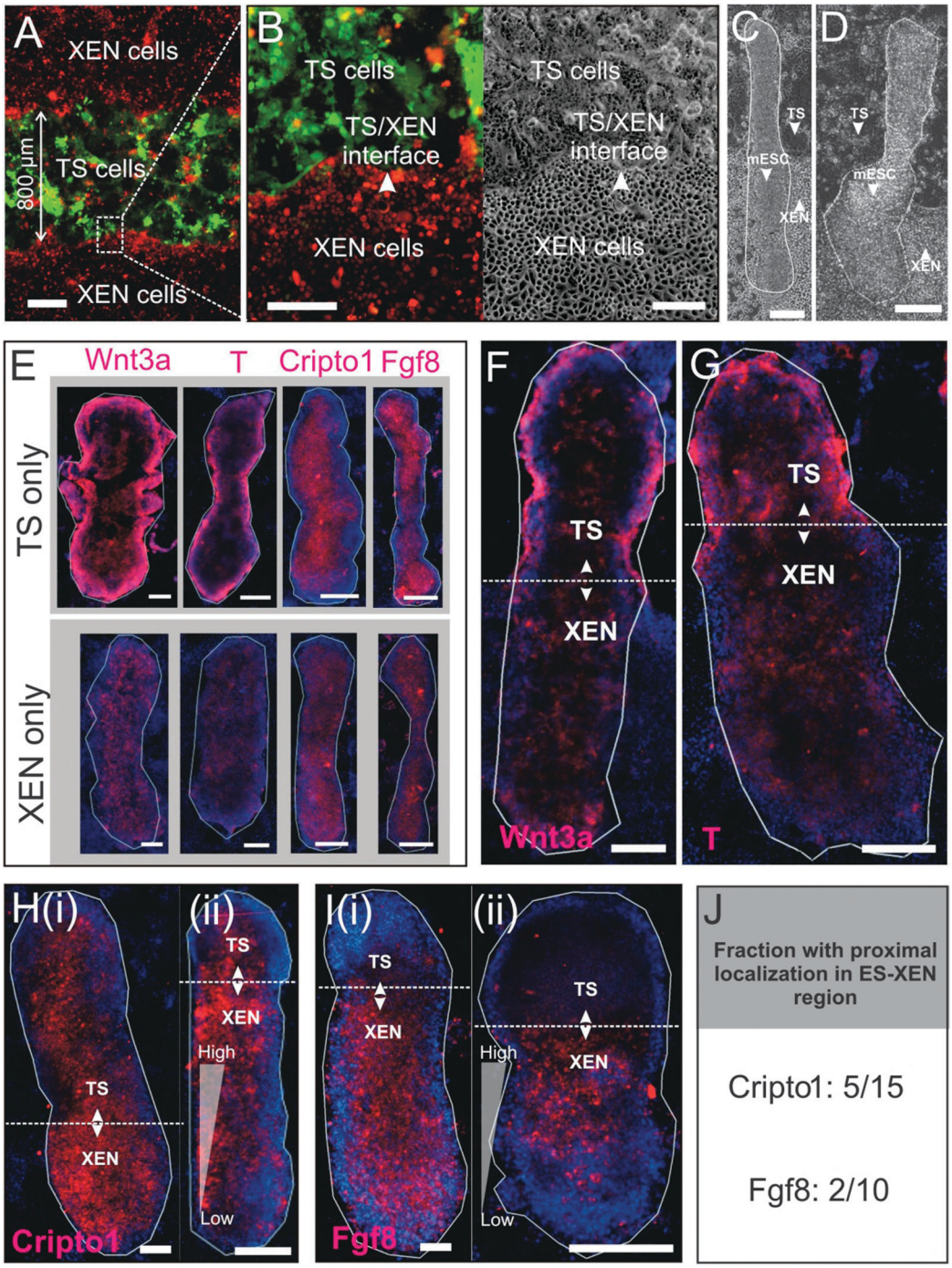

Fig. 3 *In vitro* proximal-distal (PD) epiblast patterning. (A) Micropatterned TS cells and XEN cells. (B) TS-XEN cells interface. (C-D) Phase images of mESC colonies on TS-XEN interface (C) immediately post patterning and (D) after 5 days of culture. (E) Immunofluorescence staining of proximal embryonic markers (in red) in control colonies on TS or XEN cells alone. (F–I) Immunofluorescence assessment for proximal marker (in red) polarization in δESP-patterned mESC colonies: (F) Wnt3a, (G) T, (H) Cripto1 and (I) Fgf8. Nuclei were counterstained blue. (J) Tabulation of fraction of colonies examined that exhibited polarization of Cripto1 and Fgf8 within XEN-region. Scale bars in (A) = 50 μm; scale bars in (B–I) = 200 μm.

to distal (on XEN cells) intensity ratio was used as a quantitative indicator of PD asymmetry, where a larger deviation of PD intensity ratio from 1 indicates greater asymmetry. Consistent with our qualitative assessment above, mESC colonies on either TS or XEN cells alone had a PD intensity ratio of 1 (Fig. 4C–D). In comparison, mESC colonies presented with both TS and XEN exhibited significant PD asymmetries in Wnt3a and T distribution (Fig. 4C-D), which became significantly pronounced over time (SI Fig. 8A-B). We also measured the expression of the early neuroectodermal marker, Sox1, which is indicative of anterior cell fate, with a GFP-Sox1 reporter cell line. Sox1 expression was marginally asymmetric along the

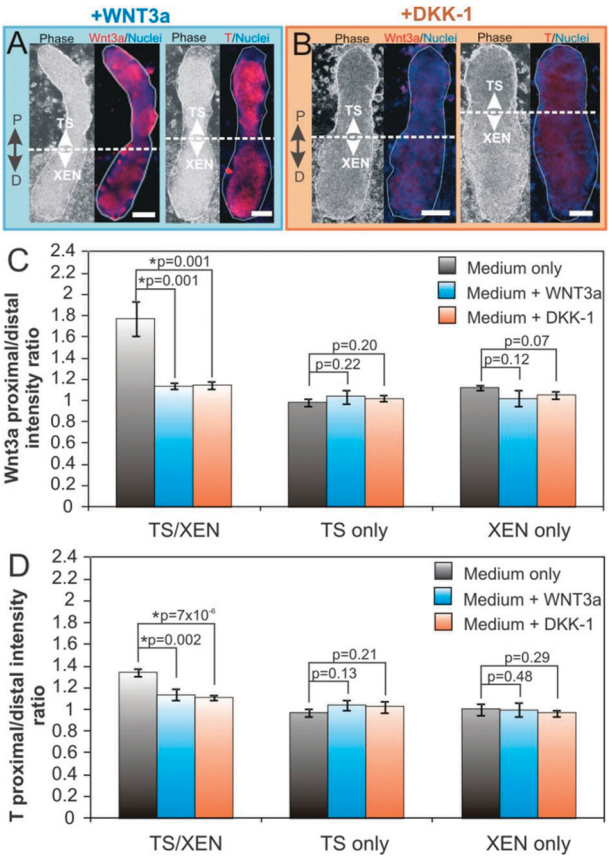

Fig. 4 PD patterning in δESP embryonic model is modulated by Wnt-signaling. Disruption of polarized Wnt3a and T expressions by exogenous (A) WNT3a (50 ng ml^{-1}) or (B) DKK-1 (200 ng ml^{-1}). Quantitative assessment of (C) Wnt3a and (D) T PD asymmetries. Data are average of >10 colonies (on TS-XEN interface) or >3 colonies (on TS or XEN cells alone) from 2 independent experiments ± s.e.m. Pairwise comparisons (*t*-test) are indicated by connecting lines. * indicates statistical significance ($p < 0.05$). Scale bars = 200 μm.

designated PD axis and remained constant over culture time (SI Fig. 8C). Hence, imposing organization of extraembryonic environments is sufficient to generate quantifiable PD patterning in mESCs, which in turn is amenable to experimental perturbations.

The observed PD asymmetries in proximal epiblast markers can be attributed at least in part to Wnt signaling gradients established by TS and XEN cells patterned along the designated PD axis since the ExE secretes soluble factors, such as BMP4, that activate Wnt signaling in the proximal epiblast.[27] We examined whether the patterning is sensitive to disruption of Wnt signaling by adding exogenous Wnt agonist (WNT3a) or antagonist (DKK-1) to the co-culture medium. Since Wnt3a and T were more robustly polarized than Cripto1 and Fgf8, we assessed their distribution in the exogenous disruption experiments after 5 days of culture. In the presence of WNT3a, Wnt3a and T expression were more pronounced (Fig. 4A), while in the presence of DKK-1, their expression was attenuated (Fig. 4B). These observations were consistent with the agonist/antagonistic functions of the exogenous factors.[28] However, PD patterning of Wnt3a and T in the mESC colonies were abolished in both cases since the PD intensity ratios of Wnt3a (Fig. 4C) and T (Fig. 4D) in colonies on TS/XEN cells were not significantly different from control colonies on TS or XEN cells alone. Sox1 distribution in the proximal and distal colony regions was not affected by the addition of WNT3a or DKK-1 (SI Fig. 9). This is corroborated by a report from Rodriguez *et al.* that absence of ExE, a source for Wnt-activating molecules that include BMP4, from the conceptus affected posterior cell fate specification but did not inhibit development of anterior Sox1-postive cells.[3]

Discussion

Pluripotent cells and stem cells in embryonic and adult tissues *in vivo* exist in structurally asymmetric environments. There is increasing evidence in embryos[1] and adult stem cell niches, notably in germline and hematopoietic stem cell systems,[2,19] that the position of a pluripotent or multipotent cell in an asymmetric architecture translates into polarization in molecular expression that determines its fate. Existing approaches for determining whether environmental spatial organization has developmental significance center around the use of live imaging to perform lineage tracing in model organisms[2,29] or ablation of a particular anatomical feature within the niche.[3] However, performing imaging and physical manipulation are challenging in mammals and late-stage embryos.[11] Even when developmentally-relevant asymmetrical stem cell microenvironments have been identified, deciphering the molecular mechanisms in a spatially asymmetric anatomical context is not trivial. Investigation into molecular signaling pathways primarily rely on knockout or transgenic organisms, which are costly and slow to produce.[6] More importantly, these molecular modulators can only be studied one at a time since disrupting multiple factors simultaneously is challenging and often lethal. Consequently, there is increasing interest to use *in vitro* stem cell cultures as complementary models to study developmental biology.[12,30]

The utility of *in vitro* models, as evident from cancer or disease models, is not to mimic a complex biological system entirely, but to distill certain aspects of the system to be studied in greater breadth and depth by leveraging their experimental accessibility *e.g.*, treatment regimes, real-time imaging, multiplexing. Hence, specific aspects of developmental processes can in principle, be identified (from animal studies) and modeled with *in vitro* models. In *in vitro* stem cell models, factors are added into the system instead of being subtracted (as in animal models), allowing questions of *sufficiency*-the minimum set of components specifying a desired cell fate to be probed. However, *in vitro* developmental models have not been widely adopted to date, in part because current models fail to incorporate spatial environmental organization, which is a key aspect of developmental processes. Monolayer cultures only allow screening for specific environmental cues (*e.g.*, ECMs, soluble factors) that instruct stem cells into various lineages.[8–10] EBs can form rudimentary organized structures[28] but the cells within are not amenable to experimental manipulation. Current methods of modulating signaling gradients in EBs such as changing EB sizes,[19] microdissection[31] and exposure to soluble factors,[28] act indirectly, confounding interpretation on variation in spatial environmental organization and cell fate instruction. δESP overcomes these limitations to enable creation of spatially

organized *in vitro* developmental models *via* reproducible establishment and manipulation of stem cell environmental asymmetries (*e.g.*, cells and ECMs). From this vantage, the PD patterning experiment provides a framework for how δESP can be useful in modeling spatially patterned differentiation in developmental processes.

δESP can be customized to match the length scale of the stem cell niche of interest. Besides stencil patterning used here, other micropatterning techniques[17] could also be employed (*e.g.*, microcontact printing), and may provide better precision for smaller features. We used the BFC to pattern stem cells onto the organized environment since BFC allows for substrate-independent patterning (*i.e.*, able to pattern on cells/ECMs)[16,32,33] and can align the stem cells to the underlying microenvironments. The accuracy of the alignment limits the feature size, and in the current δESP is ~500 μm. It is conceivable that multiple rounds of cell patterning would allow the creation of microenvironment with >3 spatially organized cell types, leading to the realization of ever-more-complex *in vitro* models.

Our results from patterning mESCs in an asymmetric microenvironment presenting both self-renewal and differentiation cue provide the first experimental evidence that the overall spatial organization of cell fates within an ESC colony is a summation of cellular responses to a local underlying environment occurring over a length scale of a few cells (Fig. 2). Next, we applied δESP to model an early developmental step and demonstrated that a fairly simplistic two-dimensional equivalent of an early mouse embryo can be generated *in vitro*. While δESP cannot fully recapitulate the three-dimensional interactions between extraembryonic tissues and the cup-like epiblast in an E5.5 mouse embryo, it can be used to test whether mimicking the relative *in vivo* spatial arrangement of the ExE, epiblast and VE induces similar differentiation asymmetry as develops in an epiblast. By presenting representative environments from the ExE and VE to a mESC colony in a PD orientation, molecular markers, such as T, Wnt3a, Cripto1 and Fgf8, which localize to the proximal end of the embryo, can similarly exhibit a PD distribution (Fig. 3), and can be measured quantitatively (Fig. 4). The disruption of these polarized distributions when exogenous Wnt agonist or antagonist were added to the system suggests that at least one of the triad of Bmp-Wnt-Nodal signaling gradients responsible for driving this developmental step *in vivo* is also active in the *in vitro* analogue.[1,4] An interesting area of future research will be to investigate whether the ExE and VE cells also adopt downstream fates during the course of the differentiation, and whether multiple sequential developmental steps could be modeled. In this regard, one advantage of a cell-based niche (in contrast to a niche comprised of soluble or matrix signals) is that the cells are active components in the system and can react to the each other.

The choice of cells used in a δESP *in vitro* model need not necessarily be restricted to the particular developmental step that one wishes to emulate, thus making the approach and technique more generalizable. For instance, the epiblast at PD axis formation is more accurately represented by epiblast stem cells (EpiSCs) than the naïve ESCs used here.[34] Indeed, it is interesting that although the three cell types (*i.e.*, TS, XEN and ES cells) used in the δESP PD patterning model are precursors to the ExE, VE and epiblast,[23,24,34] they are still capable of generating a molecular asymmetry similar to a PD axis. This suggests that the mESCs in the δESP model similarly go through an epiblast-like stage to adopt a mesoendodermal fate as previously reported.[35]

Experimental

Cell lines and maintenance

The mouse embryonic stem cell (mESC) lines used had either a GFP-Sox2 reporter (Sox2, from Rudolf Jaenisch) or GFP-Sox1 reporter (46C, from Austin Smith). Sox2 mESCs were routinely maintained in high glucose DMEM (Invitrogen) supplemented with 15% fetal calf serum (FCS) (16141079, Invitrogen), 4 mM L-glutamine (25030081, Invitrogen), 1 mM non-essential amino acid (11140050, Invitrogen), 50 units ml^{-1} penicillin, 50 μg ml^{-1} streptomycin (15140122, Invitrogen), 100 μM β-mercaptoethanol (M7522, Sigma) and 1000 units ml^{-1} leukemia inhibitory factor (LIF, ESG1107, Chemicon). 46C mESCs were maintained in GMEM (11710035, Invitrogen) supplemented with 10% FCS, 50 U/ml penicillin, 50 μg ml^{-1} streptomycin, 100 μM β-mercaptoethanol and 1000 units ml^{-1} LIF. STO fibroblasts (CRL-1503, ATCC) were maintained in high glucose DMEM supplemented with 10% FCS, 2 mM L-glutamine, 1 mM sodium pyruvate (11360-070, Invitrogen), 100 units ml^{-1} penicillin, and 100 μg ml^{-1} streptomycin.

Mouse trophoblast stem (TS) cells and extraembryonic endoderm (XEN) cells were obtained from Janet Rossant and maintained on gelatin-coated tissue culture dishes according to protocols reported in Tanaka *et al.*[23] and Kunath *et al.*[24] respectively. Briefly, TS cells were cultured in basal TS medium supplemented with 70% mouse embryonic fibroblast conditioned medium (MEF-CM), 25 ng ml^{-1} human recombinant FGF4 (235-F4-025, R&D Systems) and 1 μg ml^{-1} heparin (H3149, Sigma). Basal TS medium consisted of RPMI 1640 medium (21870, Invitrogen) supplemented with 20% FCS, 2 mM L-glutamine, 1 mM sodium pyruvate, 100 μM β-mercaptoethanol, 50 units ml^{-1} penicillin and 50 μg ml^{-1} streptomycin. XEN cells were maintained in basal XEN medium supplemented with 70% MEF-CM. Basal XEN medium has the same formulation as basal TS medium except 15% FCS was used.

Preparation of mouse embryonic fibroblast conditioned medium (MEF-CM)

Mouse embryonic fibroblasts (MEF) were maintained in high glucose DMEM supplemented with 15% FCS, 4 mM L-glutamine, 100 units ml^{-1} penicillin and 100 μg ml^{-1} streptomycin for up to 5 passages. To prepare MEF-CM, confluent MEFs were treated with 10 μg ml^{-1} mitomycin (M4287, Sigma) for 3 h and washed 3 times with PBS. The cells were cultured in basal TS medium (5 ml per 10^6 cells) for 3 days. The MEF-CM was collected, filtered and stored in −20 °C. MEFs post mitomycin treatment can be used up to 10 days for conditioned medium preparation.

Device fabrication

The components (stencil, Bio Flip Chip (BFC) and stepped gasket) for δESP were designed with AutoCAD (AutoDesk) to

ensure that the BFC wells align to the stabilized interface of stencil-patterned cells or ECMs. The dimensions of the various components are given in SI Fig. 1E. Polydimethylsiloxane (PDMS) stencils were fabricated by using a laser-cutter (Universal Laser System) to cut the designated patterns on a 127 μm thick PDMS sheet (Specialty Silicone Products Inc.) and then bonding it to a laser-cut, 2 mm thick PDMS gasket. PDMS BFCs were obtained by pouring degassed PDMS mixture (10 : 1 ratio of prepolymer to curing agent) (Sylgard 184, Dow Corning) onto a stereolithography fabricated plastic mold (Prototherm 12120, Fineline Prototyping) and allowed to cure at 60 °C overnight. The stepped PDMS gasket consisted of two 2–3 mm PDMS slabs trimmed to the specified dimensions (SI Fig. 1E) and bonded together. All components were sterilized by autoclaving at 121 °C for 20 min.

δESP for patterning reciprocal self-renewal and neural fates

STO fibroblasts were stencil-patterned onto a 60 mm polystyrene dish as 800 μm-wide strips at a density of 1.8×10^5 cells cm^{-2}. After 2 h incubation, the stencil was removed and 0.1% gelatin (ES-006-B, Millipore) in phosphate buffer saline (PBS) was added to coat the remaining substrate for 10 min. The STO fibroblasts were then treated with 10 μg ml^{-1} mitomycin (M4287, Sigma) for 3 h to arrest their proliferation, washed 3 times with PBS and incubated in STO culture medium overnight. Sox2 mESCs were resuspended in N2B27 medium, prepared according to formulation in Ying *et al.*[20] supplemented with 1000 units ml^{-1} LIF and 60 mM HEPES buffer (15630-080, Invitrogen) and patterned onto the STO/gelatin substrate using a BFC with 2 mm (L) × 200 μm (W) × 400 μm (H) wells accordingly to Rosenthal *et al.*[16] Briefly, the BFC was passivated with 0.2% bovine serum albumin (BSA) overnight before 400 μl of mESC suspension was dispensed onto it. The cells were allowed to settle into the microwells of the BFC and excess cells were removed by repeated washing with PBS. The BFC was then aligned and flipped onto the stepped gasket bounding the micropatterned STO fibroblasts and gelatin, and secured with binding clips. After overnight incubation, the BFC was removed, washed 3 times with PBS and cultured in N2B27 for 5 days with fresh medium change every 24 h. Self-renewal and neuronal differentiation markers were assessed after 5 days of differentiation by immunofluorescence staining and quantified by image processing.

δESP for patterning proximal-distal fates in mESCs

TS cells were stencil-patterned at confluence as described above and incubated for 6 h to allow for cell attachment. The stencil was removed and the remaining substrate was coated with 0.1% gelatin in PBS for 10 min. After overnight incubation in complete TS medium (*i.e.*, basal TS medium + 70% MEF-CM, FGF4, heparin), 2×10^5 XEN cells (3.47×10^4 cells cm^{-2}) were plated and incubated for 1 h. Excess unattached XEN cells were removed by washing with PBS and the TS/XEN co-culture was incubated overnight in complete TS medium for stabilization of the TS/XEN cell interface. 46C mESCs were resuspended in complete TS medium supplemented with 60 mM HEPES buffer and patterned using a BFC with 1.5 mm (L) × 160 μm (W) × 400 μm (H) wells as described above. After 6 h, the BFC was removed and the TS/XEN/mESC co-culture was maintained in a co-culture medium comprising of complete TS cell medium with 1 μg ml^{-1} recombinant mouse LIF antibody (AF449, R&D Systems) for 5 days. Fresh medium was changed every 24 h. To disrupt Wnt-signaling gradients in the TS/XEN/mESC co-culture, 50 ng ml^{-1} of recombinant mouse WNT3a (1324-WN, R&D Systems) or 200 ng ml^{-1} of recombinant mouse DKK-1 (5897-DK, R&D Systems) were added to the co-culture medium.

Immunofluorescence staining

Samples were incubated with 4% paraformaldehyde (PFA, 15710, Electron Microscopy Sciences) for 15 min, 0.5% Triton X-100 (234729, Sigma) for 15 min, Image-IT™ FX Signal Enhancer (I36933, Invitrogen) for 30 min and 10% FCS or Odessey blocking buffer (927-40000, LI-COR BioSciences) overnight at 4 °C. They were then incubated with primary antibodies overnight at 4 °C at the following concentrations diluted in blocking buffer: 0.78 μg ml^{-1} rabbit-anti-mouse Nestin (ab5968, Abcam), 4 μg ml^{-1} rabbit-anti-mouse Wnt3a (ab28472, Abcam), 4 μg ml^{-1} rabbit-anti-mouse Brachyury (T, ab20680, Abcam), 10 μg ml^{-1} rabbit-anti-Cripto1 (ab19917, Abcam), 5 μg ml^{-1} rabbit-anti-Fgf8 (ab81384, Abcam) and 10 μg ml^{-1} rabbit-anti-Lefty2 (PAB1922, Abnova). Subsequently, the samples were washed 5 times with blocking buffer (20 min between each wash) and incubated with 1 μg ml^{-1} Alexa Fluor® 532 goat-anti-rabbit IgG secondary antibody (A-11009, Molecular Probes), diluted in blocking buffer, for 1 h at room temperature. Samples were then washed 3 times with PBS and counter-stained with 10 μg ml^{-1} Hoechst 33342 (H3570, Molecular Probes) for 5 min. After rinsing with PBS and distilled water, the samples were finally mounted with an aqueous mounting medium (17985-10, Electron Microscopy Sciences) on cover glass.

Image acquisition and analysis

All images were acquired with an inverted epifluorescence microscope (Nikon Eclipse *Ti*) with an automated stage (Ludl MAC 5000). Tile-scans of entire mESC colonies were obtained with a 10X objective. The stitched images were then processed with Matlab (Mathworks) for quantification of fluorescent markers.

In the self-renewal-differentiation patterning experiment, colony regions in self-renewing (on STO fibroblasts) or differentiating (on gelatin) microenvironments were outlined manually on phase images to generate regional masks. The masks were applied onto processed (thresholding, binary conversion) fluorescent images of Sox2 expression to quantify the percentage of Sox2-positive area in the entire colony or in the respective self-renewing or differentiating colony regions. mESC colonies presented with single microenvironments (on STO fibroblasts or gelatin alone) were divided equally into two regions to serve as proxies for self-renewing and differentiating regions of colonies and processed similarly as described. The transition distance for phenotypic switch was calculated by obtaining 5 Sox2 intensity profiles in varying directions, and fitting each profile with a 4-parameter logistic function:

$$y = \frac{(a-b)}{1+\left(\frac{x}{c}\right)d}$$

where y is Sox2 fluorescence intensity, x is distance and a-d are fitted parameters) (SI Fig. 3A-B). The profile of the slope was then obtained by taking the 1st derivative of the fitted function, and the transition distance is taken to be the distance spanning 80% of the maximum slope (SI Fig. 3C).

For the PD patterning experiment, masks for mESC colony regions on TS and XEN cells were generated as described above with an additional step to erode the centre of the mask area. This generated proximal (on TS cells) or distal (on XEN cells) regional masks that cover just the colony periphery, where Wnt3a and T were localized. The regional masks were then applied to processed (contrast adjustment, thresholding based on TS and XEN cell controls for unspecific staining) fluorescent images of Wnt3a and T to quantify the average fluorescent intensities in the proximal (on TS cells) and distal (on XEN cells) colony regions.

Statistical analysis

Linear regression between Sox2 expression and ratios of self-renewal to differentiation microenvironments was performed with SigmaPlot (Systat Software Inc.). The significance of the correlation of determination (R^2) was determined by f-test (ANOVA, $n = 122$). The significance of differences in the transition distance across the 3 bins of dual microenvironment ratios (*i.e.*, <40%, 40–60% and >60% STO cells) was determined by f-test (ANOVA, $n = 30$).

An unpaired t-test was performed to determine the significance of pairwise comparisons in PD patterning experiments, $n > 10$ for test colonies and $n > 3$ for control colonies.

Conclusions

The complexity of developmental processes calls for technical innovations to probe the spatial intricacies that exist between environmental cues and stem\progenitor cell fates. δESP represents a step toward more realistically modeling the complexity that exists *in vivo*. The versatility of the resulting spatially organized *in vitro* developmental models can be generalized to capitalize on the current knowledge on cell fate instruction by environmental factors as "building blocks", which can then be spatially organized around stem cell to generate biologically meaningful stem cell microenvironments and gain further insights into organized differentiation during development.

Acknowledgements

We thank Salil Desai, Nikhil Mittal and Somponnat Sampattavanich for technical assistance. This work was supported by the NIH (EB007278), Institute of Bioengineering and Nanotechnology and A*STAR International Fellowship.

Notes and references

1 J. Rossant and P. P. L. Tam, *Development*, 2009, **136**, 701–713.
2 Y. Xie, T. Yin, W. Wiegraebe, X. C. He, D. Miller, D. Stark, K. Perko, R. Alexander, J. Schwartz, J. C. Grindley, J. Park, J. S. Haug, J. P. Wunderlich, H. Li, S. Zhang, T. Johnson, R. A. Feldman and L. Li, *Nature*, 2009, **457**, 97–101.
3 T. A. Rodriguez, S. Srinivas, M. P. Clements, J. C. Smith and R. S. P. Beddington, *Development*, 2005, **132**, 2513–2520.
4 R. S. P. Beddington and E. J. Robertson, *Cell*, 1999, **96**, 195–209.
5 D. Dupuy, N. Bertin, C. A. Hidalgo, K. Venkatesan, D. Tu, D. Lee, J. Rosenberg, N. Svrzikapa, A. Blanc, A. Carnec, A.-R. Carvunis, R. Pulak, J. Shingles, J. Reece-Hoyes, R. Hunt-Newbury, R. Viveiros, W. A. Mohler, M. Tasan, F. P. Roth, C. Le Peuch, I. A. Hope, R. Johnsen, D. G. Moerman, A.-L. Barabasi, D. Baillie and M. Vidal, *Nat. Biotechnol.*, 2007, **25**, 663–668.
6 J. Brennan, C. C. Lu, D. P. Norris, T. A. Rodriguez, R. S. P. Beddington and E. J. Robertson, *Nature*, 2001, **411**, 965–969.
7 J. Ding, L. Yang, Y.-T. Yan, A. Chen, N. Desai, A. Wynshaw-Boris and M. M. Shen, *Nature*, 1998, **395**, 702–707.
8 A. J. Engler, S. Sen, H. L. Sweeney and D. E. Discher, *Cell*, 2006, **126**, 677–689.
9 C. J. Flaim, D. Teng, S. Chien and S. N. Bhatia, *Stem Cells Dev.*, 2008, **17**, 29–39.
10 R. McBeath, D. M. Pirone, C. M. Nelson, K. Bhadriraju and C. S. Chen, *Dev. Cell*, 2004, **6**, 483–495.
11 S.-I. Nishikawa, L. M. Jakt and T. Era, *Nat. Rev. Mol. Cell Biol.*, 2007, **8**, 502–507.
12 W. Weitzer, *Embryonic Stem Cell-Derived Embryoid Bodies: An In vitro Model of Eutherian Pregastrulation Development and Early Gastrulation*, 2006.
13 R. Peerani, B. M. Rao, C. Bauwens, T. Yin, G. A. Wood, A. Nagy, E. Kumacheva and P. W. Zandstra, *EMBO J.*, 2007, **26**, 4744–4755.
14 S. Raghavan and C. S. Chen, *Adv. Mater.*, 2004, **16**, 1303–1313.
15 C. A. Goubko and X. Cao, *Mater. Sci. Eng., C*, 2009, **29**, 1855–1868.
16 A. Rosenthal, A. Macdonald and J. Voldman, *Biomaterials*, 2007, **28**, 3208–3216.
17 D. Falconnet, G. Csucs, H. M. Grandin and M. Textor, *Biomaterials*, 2006, **27**, 3044–3063.
18 R. E. Davey and P. W. Zandstra, *Stem Cells*, 2006, **24**, 2538–2548.
19 C. L. Bauwens, R. Peerani, S. Niebruegge, K. A. Woodhouse, E. Kumacheva, M. Husain and P. W. Zandstra, *Stem Cells*, 2008, **26**, 2300–2310.
20 Q.-L. Ying, M. Stavridis, D. Griffiths, M. Li and A. Smith, *Nat. Biotechnol.*, 2003, **21**, 183–186.
21 Q.-L. Ying, J. Nichols, I. Chambers and A. Smith, *Cell*, 2003, **115**, 281–292.
22 X. Qi, T.-G. Li, J. Hao, J. Hu, J. Wang, H. Simmons, S. Miura, Y. Mishina and G.-Q. Zhao, *Proc. Natl. Acad. Sci. U. S. A.*, 2004, **101**, 6027–6032.
23 S. Tanaka, T. Kunath, A.-K. Hadjantonakis, A. Nagy and J. Rossant, *Science*, 1998, **282**, 2072–2075.
24 T. Kunath, D. Arnaud, G. D. Uy, I. Okamoto, C. Chureau, Y. Yamanaka, E. Heard, R. L. Gardner, P. Avner and J. Rossant, *Development*, 2005, **132**, 1649–1661.
25 J. A. Rivera-Pérez and T. Magnuson, *Dev. Biol.*, 2005, **288**, 363–371.
26 C. Meno, A. Shimono, Y. Saijoh, K. Yashiro, K. Mochida, S. Ohishi, S. Noji, H. Kondoh and H. Hamada, *Cell*, 1998, **94**, 287–297.
27 D. A. F. Loebel, C. M. Watson, R. A. De Young and P. P. L. Tam, *Dev. Biol.*, 2003, **264**, 1–14.
28 D. ten Berge, W. Koole, C. Fuerer, M. Fish, E. Eroglu and R. Nusse, *Cell Stem Cell*, 2008, **3**, 508–518.
29 S. A. Morris, R. T. Y. Teo, H. Li, P. Robson, D. M. Glover and M. Zernicka-Goetz, *Proc. Natl. Acad. Sci. U. S. A.*, 2010, **107**, 6364–6369.
30 A. M. Wobus and K. R. Boheler, *Physiol. Rev.*, 2005, **85**, 635–678.
31 O. Kopper, O. Giladi, T. Golan-Lev and N. Benvenisty, *Stem Cells*, 2010, **28**, 75–83.
32 P. Calvert, *Science*, 2007, **318**, 208–209.
33 H. Tavana, B. Mosadegh and S. Takayama, *Adv. Mater.*, 2010, **22**, 2628–2631.
34 P. J. Tesar, J. G. Chenoweth, F. A. Brook, T. J. Davies, E. P. Evans, D. L. Mack, R. L. Gardner and R. D. G. McKay, *Nature*, 2007, **448**, 196–199.
35 T. Graf and M. Stadtfeld, *Cell Stem Cell*, 2008, **3**, 480–483.